BMC Chemical Engineering

RESEARCH ARTICLE Open Access

Incorporation of Cu_3BTC_2 nanocrystals to increase the permeability of polymeric membranes in O_2/N_2 separation

Chong Yang Chuah[1] and Tae-Hyun Bae[1,2*]

Abstract

To increase permeability in O_2/N_2 separation without compromising selectivity, Cu_3BTC_2 (or HKUST-1) nanocrystals, which possess well-defined channels and high surface area, were used as the filler for mixed-matrix membrane fabrication. The Cu_3BTC_2 nanocrystals, which were synthesized at room temperature with a facile method, showed desirable physical properties and porosity comparable to those of a commercial Cu_3BTC_2 adsorbent (Basolite C300). High-quality mixed-matrix membranes without appreciable defects were successfully fabricated with both Matrimid and polysulfone, which are commercial membrane polymers that suffer from poor permeability. Gas permeation testing revealed that 20 wt% Cu_3BTC_2 nanocrystals loading dramatically improved the O_2 permeability of both polymer membranes (106% for Matrimid and 379% for polysulfone), with modest increases in O_2/N_2 selectivity. A detailed analysis of diffusivity and solubility showed that the overall O_2/N_2 diffusion selectivity was improved substantially over that of a neat polymeric membrane with the incorporation of Cu_3BTC_2 nanocrystals. A comparative study with literature data demonstrated that Cu_3BTC_2 nanocrystals are far more effective than other metal-organic framework fillers tested to increase permeability in O_2/N_2 separation.

Keywords: O_2/N_2 separation, Cu_3BTC_2, Mixed-matrix membrane, Metal-organic framework, Permeability, Diffusivity

Introduction

There is growing interest in oxygen-enhanced combustion as a tool to improve energy efficiency in combustion processes typically used in energy production [1, 2]. In general, traditional fuel combustion typically uses air (21% O_2 and 79% N_2) as the oxidant, and such an approach is the simplest way of energy generation. However, nitrogen, which is the largest component of air but does not participate in the combustion reaction, takes up a large amount of heat in combustion processes, leading to a drastic decrease in energy efficiency [1, 2]. This decrease is exacerbated by the possible production of nitrogen oxides (NO_x), which have negative consequences on the environment such as photochemical smog and acid rain. Thus, the O_2 content in the feed source must be increased to increase the efficiency of the energy output and to decrease emissions of carbon monoxide, particulates, and smoke due to incomplete combustion [3, 4]. This strategy has been applied to CO_2 capture processes as well. A so-called oxy-fuel combustion process, in which pure O_2 is used as the oxidant, produces CO_2 gas saturated with water vapor as the byproduct [5]. Thus, after condensing the water, pure CO_2 gas can be ready for sequestration or utilization processes.

In this regard, many approaches have been developed to produce an oxygen-enriched stream for these processes. To date, technologies such as cryogenic air distillation and adsorption have been well studied for O_2/N_2 separation [6]. Nonetheless, the high energy penalties on these two processes limit their potential practicability in O_2/N_2 separation. Thus, unlike conventional separation processes, membrane-based separation provides advantages such as a smaller footprint and high energy efficiency [7]. However, conventional polymeric membranes, which possess high processability and mechanical stability, show limited performance as demonstrated by the permeability–selectivity trade-off in the Robeson plot [8–10]. However, porous crystalline membranes such as zeolites and

* Correspondence: thbae@ntu.edu.sg
[1]School of Chemical and Biomedical Engineering, Nanyang Technological University, Singapore 637459, Singapore
[2]Singapore Membrane Technology Centre, Nanyang Environment and Water Research Institute, Nanyang Technological University, Singapore 637141, Singapore

metal-organic frameworks (MOFs) suffer from poor scalability that hampers the large-scale production of high-quality membranes [11]. Hence, mixed-matrix membranes (composite membranes) have been proposed as a technically viable option to enhance the permeability and selectivity of polymer membranes while retaining the advantages of polymeric materials [12, 13]. In essence, microporous materials, namely, zeolites, MOFs, carbon molecular sieves, and microporous organic polymers have been commonly incorporated into polymeric membranes to improve the gas separation performance.

To date, MOFs have attracted substantial interest among researchers in the use of these materials in mixed-matrix membranes because of their large accessible surface areas and pore volumes. Also, the functionalities can be tuned appropriately via pre- and post-synthetic functionalization depending on their potential use [14, 15]. Furthermore, MOFs typically demonstrate better compatibility with polymers owing to the presence of organic moieties [16, 17], thus eliminating the compatibilizers needed to allow better adhesion between the filler and the polymer interface, which is commonly observed when zeolite is used as the filler [18, 19]. Nonetheless, effective segregation between N_2 and O_2 is difficult to achieve in view of the comparable kinetic diameters of N_2 and O_2 (3.64 Å and 3.46 Å, respectively); the pore apertures that are present in MOFs allow these gases to propagate through these channels with ease, leading to an increase in both O_2 and N_2 permeabilities in mixed-matrix membranes [20].

In this work, we chose Cu_3BTC_2 (also known as HKUST-1) as the filler, which can effectively improve the O_2/N_2 separation performance of polymer membranes because of the following reasons. First, Cu_3BTC_2 possesses well-defined large 9 × 9 Å square pores, which allow the rapid transport of O_2 in the mixed-matrix membrane [21]. Second, the synthesis of Cu_3BTC_2 nanocrystals, which are critical for the fabrication of mixed-matrix membranes, can be readily done with a facile and scalable method. It should be noted that Cu_3BTC_2 has been commercialized under the trade name Basolite C300. However, the crystal size of Basolite C300, which is about 30 μm [Fig. 2(a)], is deemed unsuitable for membrane fabrication. Downsizing the filler materials is especially critical when the dense films made in the lab-scale study (i.e. mixed-matrix membrane) translate into large-scale asymmetric membranes in which a thin skin layer (< 1 μm) must be formed to ensure a high gas flux without appreciable interfacial defects between the filler and polymer. Meanwhile, conventional membrane polymers, namely, Matrimid and polysulfone, which suffer from low gas permeability despite their decent gas selectivities, were chosen as the polymer matrices. With the use of Cu_3BTC_2 nanocrystals as the filler material, we aimed to demonstrate a dramatic enhancement in the gas permeability without compromising the selectivity, which can in turn improve the economic feasibility of a membrane-based O_2/N_2 separation process.

Results and discussion

Synthesis of Cu_3BTC_2 nanocrystals

The successful synthesis of Cu_3BTC_2 nanocrystals was first confirmed using PXRD, as shown in Fig. 1(a). In general, identical XRD patterns were observed upon comparing the corresponding peaks of nanocrystalline Cu_3BTC_2 and Basolite C300 [22]. The corresponding peaks were also comparable with the results from the literature. However, the synthesis of Cu_3BTC_2 nanocrystals typically showed significant peak broadening on the XRD pattern as compared to the bulk crystal, which is typical behavior in the formation of smaller crystals. This behavior was further verified from the FESEM images, where nanocrystalline Cu_3BTC_2 indeed yielded smaller crystals as compared to Basolite C300, as shown in Fig. 2. The crystal size of the Basolite C300 was estimated to be 30 μm, whereas the crystal size of Cu_3BTC_2 nanocrystals was observed to range from 100 to 200 nm.

Further analyses were conducted to verify the successful formation of Cu_3BTC_2 nanocrystals. For instance, the pore characteristics of nanocrystalline Cu_3BTC_2 were comparable to those of Basolite C300, as indicated in Fig. 1(b), and Table 1 shows the surface areas and pore volumes calculated based on the physisorption isotherms. FT-IR analysis, however, confirmed the formation of Cu_3BTC_2 nanocrystals, with the successful coordination of trimesic acid into the $Cu_2(COO)_4$ paddle wheel. The formation of smaller crystals also did not sacrifice the thermal stability of the framework, in which all samples depicted the same thermal stability at 350 °C. As mentioned in the introduction, the synthesis of small crystals is typically required for the fabrication of thin and dense mixed-matrix membranes. Therefore, the synthesized nanocrystalline Cu_3BTC_2 was used in this study for the fabrication of mixed-matrix membranes.

O_2 and N_2 adsorption on Cu_3BTC_2 nanocrystals

The O_2 and N_2 adsorption isotherms of nanocrystalline Cu_3BTC_2 were measured at 35 °C, and the results were plotted as shown in Fig. 3. Large square pore windows (9 × 9 Å) in Cu_3BTC_2 allowed both adsorbates to freely access the adsorption sites in the adsorbent without any resistance. In general, because of weak interactions between both adsorbates and the Cu_3BTC_2 nanocrystals, linear adsorption isotherms were observed for both O_2 and N_2 at the pressure range we tested. Slightly higher N_2 adsorption was observed as compared to O_2 uptake because of the higher polarizability of N_2 (17.6×10^{-25} cm^3) than that of O_2 (15.4×10^{-25} cm^3) [20]. Nevertheless, the O_2/N_2 sorption selectivity of Cu_3BTC_2 can be considered negligible.

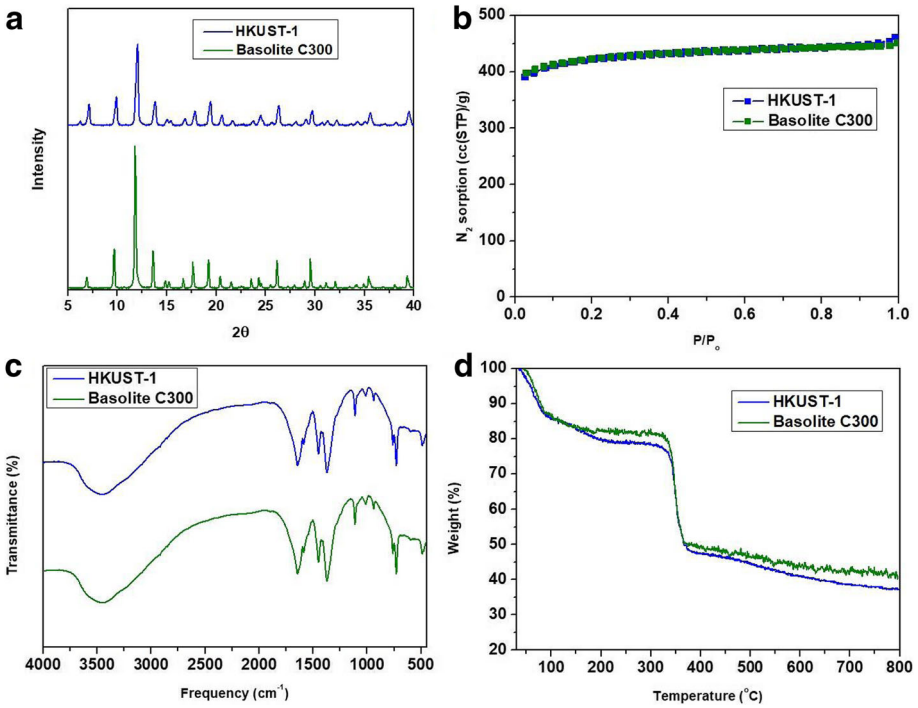

Fig. 1 **a** PXRD patterns; (**b**) N_2 physisorption isotherms; (**c**) FT-IR; and (**d**) TGA analysis of Basolite C300 and nanocrystalline Cu_3BTC_2

Fabrication of mixed-matrix membranes

In this work, two commercial polymers (Matrimid and polysulfone), which are commonly used as gas separation membranes, served as the polymer matrices for the fabrication of mixed-matrix membranes. The properties of the pure polymer were verified first using FT-IR spectroscopy (Additional file 1: Figure S1) to compare the polymer's properties with those reported in the literature [23, 24]. Mixed-matrix membranes containing 10 wt% and 20 wt% Cu_3BTC_2 nanocrystals were then fabricated, and the morphologies of these membranes were observed using FESEM (Fig. 4). As a whole, a typical "*sieve-in-a-cage*" morphology, which is commonly observed in zeolite-based mixed-matrix membranes, was not observed in this study [18, 19, 25]. The presence of organic moieties in nanocrystalline Cu_3BTC_2 allows better compatibility between the polymer chains and the filler. In addition, the use of Cu_3BTC_2 nanocrystals is desirable to increase the accessible surface area between the polymer and filler, resulting in better dispersion of fillers in the polymer matrix. The TGA analysis of the mixed-matrix membrane in comparison with the pure polymeric membranes indicated that the presence of the fillers did not affect the thermal stability of the polymer (Additional file 1: Figure S2).

Gas permeation properties

Table 2 summarizes the gas permeation properties of the membranes, which were measured at 35 °C under 1 bar

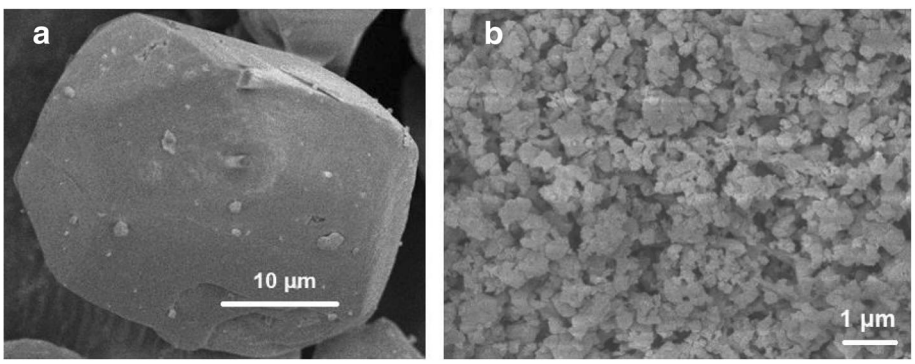

Fig. 2 FESEM images of (**a**) Basolite C300; and (**b**) nanocrystalline Cu_3BTC_2

Table 1 Surface areas and pore volumes of Basolite C300 and nanocrystalline Cu_3BTC_2 computed based on the N_2 physisorption at 77 K

Sample	S_{BET}[a] (m^2/g)	S_{LANG}[a] (m^2/g)	S_{micro}[b] (m^2/g)	V_{micro}[b] (cc/g)	V_{total}[c] (cc/g)
Basolite C300	1438	1871	0.641	1387	0.699
Cu_3BTC_2	1425	1872	0.639	1374	0.715

Note: [a] Brunauer–Emmett–Teller (BET) and Langmuir surface area were calculated based on $P/P_o = 0.05–0.2$; [b] Micropore surface area and volume were calculated using the t-plot method, based on $P/P_o = 0.4–0.6$; [c] Total pore volume was calculated at $P/P_o = 0.99$

upstream pressure with an O_2/N_2 (21:79) binary mixture. The O_2 permeability dramatically increased upon the incorporation of Cu_3BTC_2 nanocrystals into the polymer membranes, with modest enhancement in O_2/N_2 selectivity for both membranes. The best performance was observed for the 20 wt% Cu_3BTC_2/polysulfone membrane, where the O_2 permeability and O_2/N_2 selectivity increased by 379 and 11%, respectively, over the performance of the pure polysulfone membrane. Such an effect was presumably a result of the fact that the incorporation of Cu_3BTC_2 nanocrystals that possess large pore windows and well-defined pore channels allow the rapid transport of both O_2 and N_2 molecules in the mixed-matrix membrane. Nonetheless, an observable increase in selectivity in the mixed-matrix membrane as compared to that of the pristine polymer indicates that high-quality membranes without interfacial defects were successfully made with Cu_3BTC_2 nanocrystals and both polymers.

Additional evaluation of the improved permeability and selectivity of the mixed-matrix membranes was then conducted by quantifying the diffusivity and solubility of O_2 and N_2 in the mixed-matrix membranes. To this end, O_2 and N_2 adsorptions on the pure polymeric and mixed-matrix membranes were measured at 35 °C, and the results are shown in Fig. 5. The diffusivity and solubility of O_2 and N_2 were then calculated (Table 3). For both membranes, O_2 and N_2 adsorption on the mixed-matrix membrane was greater than that of the neat polymeric membranes because the Cu_3BTC_2 nanocrystals have a greater porosity and thus a higher concentration of adsorption sites than the polymers. This indicates that the presence of Cu_3BTC_2 nanocrystals increased the solubility of both O_2 and N_2 in the membranes, which is quantified in Table 3. The analysis also reveals that the Cu_3BTC_2 nanocrystals dramatically improved the diffusivities of both gases in the membranes. Hence, the increase in permeability in mixed-matrix membranes is ascribed to the increase in both the solubility and diffusivity upon incorporation of Cu_3BTC_2 nanocrystals. It was found that the O_2/N_2 sorption selectivity slightly decreased in the mixed-matrix membrane, which is consistent with the gas uptake property of the Cu_3BTC_2 nanocrystals (Fig. 3), which preferentially take up N_2 over O_2. However, the Cu_3BTC_2 nanocrystals proved to be capable of improving the diffusion selectivity, leading to an increase in O_2/N_2 permselectivity overall.

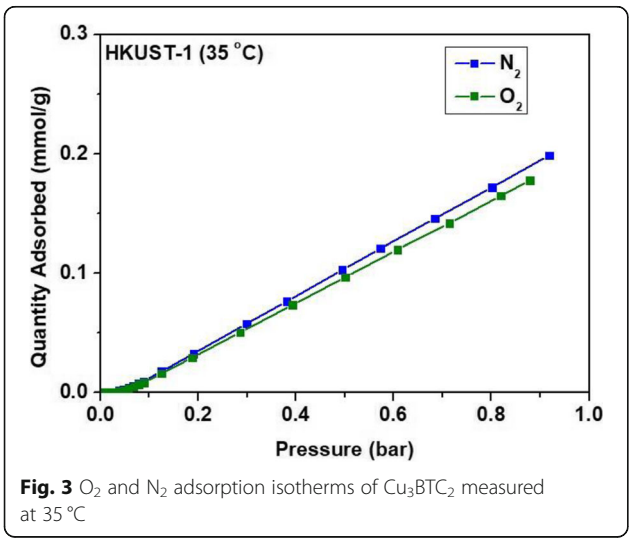

Fig. 3 O_2 and N_2 adsorption isotherms of Cu_3BTC_2 measured at 35 °C

Comparison of gas separation performance

The performance of our mixed-matrix membranes was further compared and evaluated with available literature data for effective benchmarking. Besides, the performance of the studied membranes were compared with the Robeson upper bound for comparison (Additional file 1: Figure S3). As demonstrated in Table 4, the Cu_3BTC_2 nanocrystals more effectively improved the O_2 permeability of the polymer membrane (379% for 20 wt% Cu_3BTC_2/polysulfone) than any other MOF filler tested to date. It is necessary to note that most of the performance reported to date generally determines the O_2/N_2 separation performance by the pure-component measurement, where the competition of two gases with similar properties is neglected. Thus, studying the permeability and selectivity in a mixed-gas configuration, which was used in this study, is generally more relevant for prediction of the overall gas separation performance. It is also noteworthy that such enhancement was realized with the modest enhancement in O_2/N_2 selectivity, indicating that the nonselective bypass through the filler–polymer interface was effectively controlled via good adhesion between the Cu_3BTC_2 nanocrystals and the polymers.

Conclusions

Cu_3BTC_2 nanocrystals, which have well-defined pore channels and a large surface area, were selected as the filler to improve the O_2/N_2 separation performance of polymeric membranes. It was found that the incorporation of

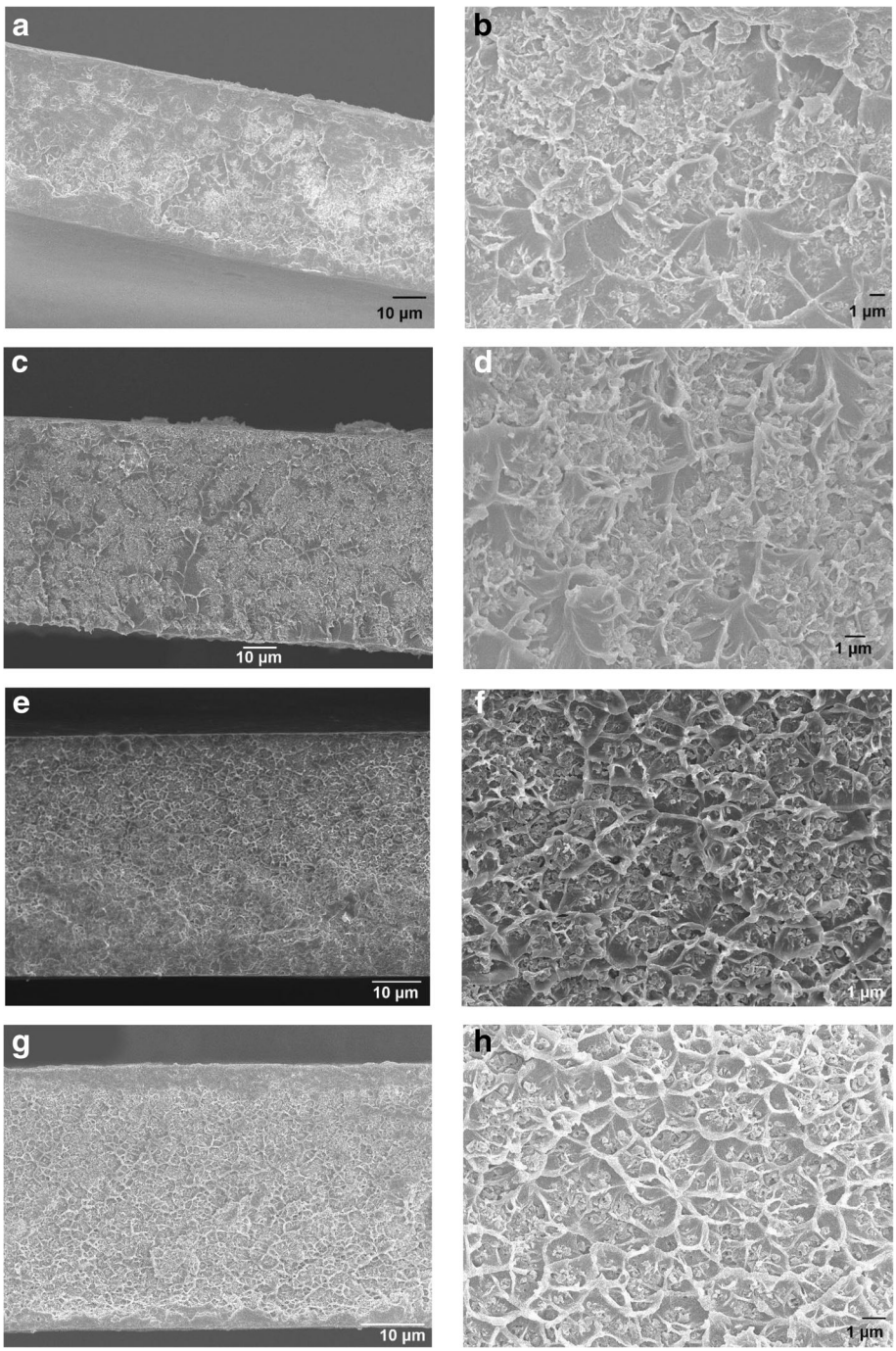

Fig. 4 FESEM images of mixed-matrix membranes for (**a**, **b**) 10 wt% Cu_3BTC_2 with polysulfone; (**c**, **d**) 20 wt% Cu_3BTC_2 with polysulfone; (**e**, **f**) 10 wt% Cu_3BTC_2 with Matrimid; and (**g**, **h**) 20 wt% Cu_3BTC_2 with Matrimid

Cu_3BTC_2 nanocrystals dramatically improved the O_2 permeability of polysulfone and Matrimid, which are widely used membrane polymers that suffer from poor permeability. A modest increase in O_2/N_2 selectivity was observed for the mixed-matrix membranes, indicating that the formation of defects at filler–polymer interfaces was effectively restricted owing to the good adhesion between the two phases. Detailed analysis reveals that the Cu_3BTC_2 nanocrystals effectively increased both diffusivity and selectivity. The O_2/N_2 diffusion selectivity was also improved by the incorporation of Cu_3BTC_2 nanocrystals, resulting in an increase in the overall O_2/N_2 permselectivity of the mixed-matrix membrane. A comparative study with literature data demonstrated that Cu_3BTC_2 nanocrystals are the

Table 2 Permeation results of pure polymer and mixed-matrix membrane under 1 bar of upstream pressure with air (21/79 O_2/N_2) at 35 °C

Membrane	O_2 permeability (barrier)	% Enhancement	O_2/N_2 selectivity	% Enhancement
Polysulfone	2.01 ± 0.12	–	4.23 ± 0.25	–
Polysulfone + 10 wt% Cu_3BTC_2	3.80 ± 0.12	89	4.85 ± 0.10	15
Polysulfone + 20 wt% Cu_3BTC_2	9.62 ± 0.58	379	4.71 ± 0.08	11
Matrimid	2.72 ± 0.27	–	5.97 ± 0.06	–
Matrimid + 10 wt% Cu_3BTC_2	4.12 ± 0.29	52	6.13 ± 0.38	3
Matrimid + 20 wt% Cu_3BTC_2	5.59 ± 0.37	106	6.18 ± 0.21	4

most effective MOF filler for improving permeability in O_2/N_2 separation. All our results suggest that incorporating Cu_3BTC_2 filler is a promising approach to improve the performance of conventional polymeric membranes for O_2/N_2 separation. Future efforts should be devoted to translating current dense membranes into asymmetric hollow fiber membranes comprising a thin skin layer made up with dense polymer layer and Cu_3BTC_2 nanocrystals.

Methods

Materials

Basolite C300, copper(II) nitrate trihydrate [$Cu(NO_3)_2{\cdot}3H_2O$], and trimesic acid ($C_9H_6O_6$) were purchased from Sigma Aldrich. Absolute ethanol and chloroform were purchased from VWR. Matrimid 5218 and polysulfone Udel® polymer were purchased from Huntsman Corporation and Solvay Special Chemicals, respectively. All chemicals were used as received without further purification.

Synthesis of Cu_3BTC_2 nanocrystals

The synthesis of Cu_3BTC_2 nanocrystals was conducted based on the procedure described elsewhere [21]. $Cu(NO_3)_2{\cdot}3H_2O$ (1.2 g) was added to 20 mL of ethanol absolute, followed by 0.6 g of $C_9H_6O_6$. The resulting mixture was stirred vigorously at room temperature for 24 h. The precipitate was obtained via vacuum filtration and washed with copious amounts of an ethanol:water mixture at a ratio of 1:1.

Membrane fabrication

A dense film of mixed-matrix membrane was fabricated via the solution-casting technique. First, nanocrystalline Cu_3BTC_2 was dispersed in chloroform using a sonication horn. The polymers were added to the solution while stirring vigorously. The mixture was stirred for 1 day to allow the solution to homogenize. The doped solution was then cast onto a glass plate using a casting knife.

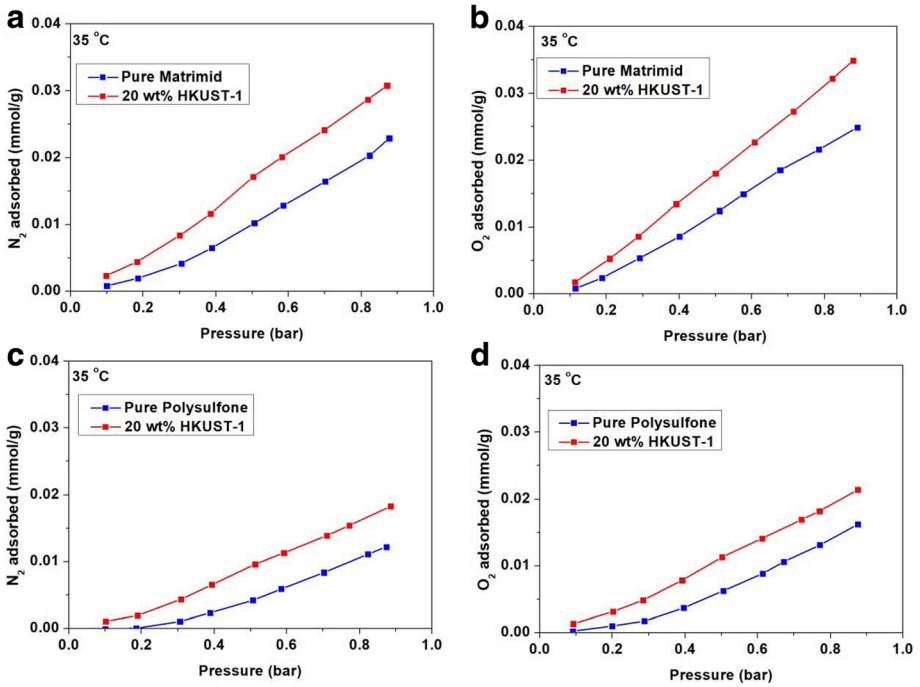

Fig. 5 Pure-component adsorption isotherms of pure polymer and mixed-matrix membranes for (**a**, **c**) N_2 and (**b**, **d**) O_2

Table 3 O_2 and N_2 solubility and diffusivity data for pure polymer and mixed-matrix membranes at 35 °C

Membrane	Density (g/cm^3)	O_2 solubility, (mol/m^3-bar)	O_2 diffusivity, × 10^{-13} (m^2/s)	N_2 solubility, (mol/m^3-bar)	N_2 diffusivity, × 10^{-13} (m^2/s)	Sorption selectivity	Diffusion selectivity
Polysulfone	1.240	19.1	7.98	14.3	2.53	1.34	3.16
Polysulfone + 20 wt% Cu_3BTC_2	1.254	29.0	23.6	24.2	6.01	1.20	3.94
Matrimid	1.200	31.4	6.58	27.7	1.25	1.13	5.26
Matrimid + 20 wt% Cu_3BTC_2	1.280	48.3	8.79	43.8	1.57	1.10	5.60

The casting environment was controlled by using a glove bag filled with chloroform vapor to prevent rapid solvent evaporation. The resulting membranes were further annealed in vacuum oven at 160 °C for 24 h before permeation testing. Thickness of typical dense membranes prepared in this work was ranged in 40 to 50 μm.

Characterization

Characterization of Cu_3BTC_2 nanocrystals and Basolite C300

The O_2 and N_2 adsorption properties of the Cu_3BTC_2 nanocrystals were measured with a volumetric gas sorption analyzer (Quantachrome, Isorb HP1). Before measurement, the Cu_3BTC_2 nanocrystals were activated at 160 °C for 8 h under high vacuum to ensure that any residual solvents that could be present in the samples were effectively removed. The isotherms, which were precisely regulated by a water circulator, were measured in the range of 0 to 1 bar at 35 °C. The porosity properties of the Cu_3BTC_2 nanocrystals and Basolite C300 were verified using N_2 physisorption analysis using a volumetric analyzer at the liquid nitrogen temperature (Quantachrome, Autosorb 6B). Similarly, Cu_3BTC_2 nanocrystals were activated under the same conditions mentioned above. The powdered X-ray diffraction (PXRD) data was obtained using a Bruker D2 phaser equipped with Cu Kα radiation. The analysis was conducted under ambient condition in the range of 2θ from 5° to 40°

Table 4 Summary of selected gas permeation data of mixed-matrix membranes that use MOFs as the filler[a]

Filler		Polymer	Filler loading (wt%)	Separation performance							Ref.
MOF	Particle size (nm)			Testing condition			$P(O_2)$ (barrier)	Permeability enhancement (%)	α (O_2/N_2)	Selectivity enhancement (%)	
				Pres. (bar)	Temp. (° C)	O_2/N_2 feed ratio[b]					
Cu-bpy-hfs	200	Matrimid	40	3.9	35	Pure	3.1	107	6.3	-5	[26]
CuTPA	66,000[c]	Poly(vinyl acetate)	15	–	–	Pure	0.62	22	6.8	3	[27]
Cu_3BTC_2	-[d]	Polysulfone	10	–	–	Pure	2.5	47	2.5	−42	[28]
MANS-1 (Ni)	640	Polysulfone	8	3	30	Pure	1.7	13	1.6	−73	[29]
MIL-53 (Al)	-[d]	Polysulfone	8	30	3	Pure	1.7	13	4.3	−27	[29]
MIL-101 (Cr)	370	Polysulfone	8	3	30	Pure	2.5	67	5.4	−37	[29]
MIL-101 (Cr)	1000	Polyurethane ether	28	4	25	Pure	9.7	246	4.2	5	[30]
MIL-101 (Fe)	950	Polysulfone	8	3	30	Pure	2.0	36	5.8	−2	[29]
Mn $(HCOO)_2$	-[d]	Polysulfone	10	–	–	Pure	1.1	−27	5.5	9	[28]
MOF-5	100	Matrimid	30	2	35	Pure	4.1	116	7.9	4	[31]
MOF-508a (Zn)	540	Polysulfone	8	3	30	Pure	1.7	13	3.7	−37	[29]
UiO-66 (Zr)	400	Polyurethane ether	28	4	25	Pure	6.1	118	5.5	38	[30]
Cu_3BTC_2	200	Polysulfone	20	1	35	21/79	9.6	379	4.7	11	This work
Cu_3BTC_2	200	Matrimid	20	1	35	21/79	5.6	106	6.2	4	This work

Note:
[a] The performance of mixed-matrix membrane was selected based on the most optimal performance in terms of O_2 permeability and/or O_2/N_2 selectivity
[b] The term "Pure" for the O_2/N_2 feed ratio refers to pure-component measurements. The selectivity is calculated based on pure-component O_2 and N_2 permeabilities
[c] Based on optical micrograph
[d] No information on the particle size

at a step size of 0.02°. The morphology of the Cu_3BTC_2 nanocrystals and Basolite C300 were observed with a field-emission scanning electron microscope (FESEM; JEOL, JSM6701) under an acceleration voltage of 5 kV.

Characterization of mixed-matrix membranes containing Cu_3BTC_2 nanocrystals

The cross sections of the mixed-matrix membranes containing Cu_3BTC_2 nanocrystals were observed using FESEM under an acceleration voltage of 5 kV. Before the observation, the membranes were cryogenically fractured in liquid nitrogen before gold coating. The properties of the pure polymeric membrane were verified from Fourier-transform–infrared spectroscopy (FT-IR) spectra with a resolution of $4\,cm^{-1}$ between 4000 and $500\,cm^{-1}$ (PerkinElmer, Spectrum One). The thermal properties of the membranes were measured using a thermogravimetric analyzer (SDT Q600 TGA, TA Instrument) at a heating rate of 10 °C/min in a temperature range from 40 °C to 800 °C under pure nitrogen purging of 100 mL/min. The densities of the pure polymeric and mixed-matrix membranes were determined based on the Archimedes principle by measuring the mass of the sample in air and in an auxiliary liquid (ethanol) using an analytical balance (Mettler Toledo, ME204) equipped with a density kit.

Mixture gas permeation test

Gas permeation tests were carried out using a constant pressure–variable volume system developed by GTR Tec Corporation. Compressed air ($O_2/N_2 = 21/79$) and helium, which were used in the system, were purchased from Airliquide. After mounting the membrane onto the permeation cell, the upstream and downstream sides were subjected to compressed air and helium gas, respectively, in which the flow rate was controlled using a mass flow controller. The downstream gas that permeated through the membrane was swept by helium at a periodic time interval until the concentrations of O_2 and N_2 reached a steady state (no significant fluctuation of their respective concentrations). The concentrations of O_2 and N_2 gas were determined from gas chromatography. The temperature of the permeation cell was set at 35 °C. The reproducibility of the permeation results was further tested by repeating the measurement for at least three samples of each polymeric and mixed-matrix membrane.

Gas adsorption analysis

To calculate the solubility–diffusivity behavior in the mixed-matrix membrane, the gas sorption of the polymeric and mixed-matrix membranes was measured with a volumetric gas sorption analyzer, as mentioned in Section 2.4.1. All membranes were measured and activated under the same conditions, as mentioned above. The O_2 or N_2 adsorption at the specified pressure was determined by fitting the curve with a linear isotherm. The solubility of O_2 and N_2 in the membrane, S, was then computed by using the relationship below:

$$S = \frac{q\rho}{p}$$

Here, q is the gas sorption per mass of the membrane, p is the pressure, and ρ is the density of the membrane. The calculation of diffusivity, D, was computed by dividing the permeability, P, by the solubility, S. The units for P and S are expressed as $mol \cdot m/m^2 \cdot s \cdot bar$ and $mol/m^3 \cdot bar$, respectively.

Additional file

Additional file 1: Supplementary Information for "Incorporation of Cu_3BTC_2 nanocrystals to increase the permeability of polymeric membranes in O_2/N_2 separation". Additional characterizations of pure polymers and mixed-matrix membranes (FTIR, TGA) as well as the comparison of membrane performance with the Robeson upper bound. (DOCX 102 kb)

Acknowledgements
Not applicable.

Funding
This research is supported by the National Research Foundation, Prime Minister's Office, Singapore, and the National Environment Agency, Ministry of the Environment and Water Resources, Singapore, under the Waste-to-Energy Competitive Research Programme (WTE CRP 1601 105). The funding body allowed us to purchase raw materials for the study but did not have any role in the design of the study and collection, analysis, and interpretation of data and in writing manuscript.

Availability of data and materials
Data repositories are not applicable for this manuscript.
Additional characterizations of pure polymer and mixed-matrix membrane is provided in the supporting information.

Authors' contributions
CYC conducted most of the experiments in this paper. T-HB contributed to the design of the experiment and data analysis. Both authors have given the approval to the final version of the manuscript.

Authors' information
Not applicable

Competing interests
The authors declare that they have no competing interests.

Publisher's Note

Received: 26 September 2018 Accepted: 2 January 2019
Published online: 30 January 2019

References
1. Baskar P, Senthilkumar A. Effects of oxygen enriched combustion on pollution and performance characteristics of a diesel engine. Eng Sci Technol Int J. 2016;19:438–43.
2. Baukal CE Jr. Oxygen-enhanced combustion. Washington D.C: CRC press; 2010.
3. Beltrame A, Porshnev P, Merchan-Merchan W, Saveliev A, Fridman A, Kennedy L, Petrova O, Zhdanok S, Amouri F, Charon O. Soot and NO formation in methane–oxygen enriched diffusion flames. Combust Flame. 2001;124:295–310.

4. Murphy JJ, Shaddix CR. Combustion kinetics of coal chars in oxygen-enriched environments. Combust. Flame. 2006;144:710–29.
5. D'Alessandro DM, Smit B, Long JR. Carbon dioxide capture: prospects for new materials. Angew Chem Int Ed. 2010;49:6058–82.
6. Murali RS, Sankarshana T, Sridhar S. Air separation by polymer-based membrane technology. Sep Purif Technol. 2013;42:130–86.
7. Wang H, Werth S, Schiestel T, Caro J. Perovskite hollow-Fiber membranes for the production of oxygen-enriched air. Angew Chem Int Ed. 2005;44:6906–9.
8. Robeson LM. Correlation of separation factor versus permeability for polymeric membranes. J Membr Sci. 1991;62:165–85.
9. Robeson LM. The upper bound revisited. J Membr Sci. 2008;320:390–400.
10. Swaidan R, Ghanem B, Pinnau I. Fine-tuned intrinsically ultramicroporous polymers redefine the permeability/selectivity upper bounds of membrane-based air and hydrogen separations. ACS Macro Lett. 2015;4:947–51.
11. Pera-Titus M. Porous inorganic membranes for CO_2 capture: present and prospects. Chem Rev. 2013;114:1413–92.
12. Chung T-S, Jiang LY, Li Y, Kulprathipanja S. Mixed matrix membranes (MMMs) comprising organic polymers with dispersed inorganic fillers for gas separation. Prog Polym Sci. 2007;32:483–507.
13. Gong H, Chuah CY, Yang Y, Bae T-H. High performance composite membranes comprising $Zn(pyrz)_2(SiF_6)$ nanocrystals for CO_2/CH_4 separation. J Ind Eng Chem. 2018;60:279–85.
14. Montoro C, García E, Calero S, Pérez-Fernández MA, López AL, Barea E, Navarro JA. Functionalisation of MOF open metal sites with pendant amines for CO_2 capture. J Mat Chem. 2012;22:10155–8.
15. Planas N, Dzubak AL, Poloni R, Lin L-C, McManus A, McDonald TM, Neaton JB, Long JR, Smit B, Gagliardi L. The mechanism of carbon dioxide adsorption in an alkylamine-functionalized metal–organic framework. J Am Chem Soc. 2013;135:7402–5.
16. Yang Y, Goh K, Wang R, Bae T-H. High-performance nanocomposite membranes realized by efficient molecular sieving with CuBDC nanosheets. Chem Commun. 2017;53:4254–7.
17. Samarasinghe S, Chuah CY, Yang Y, Bae T-H. Tailoring CO_2/CH_4 separation properties of mixed-matrix membranes via combined use of two-and three-dimensional metal-organic frameworks. J Membr Sci. 2018;557:30–7.
18. Bae T-H, Liu J, Thompson JA, Koros WJ, Jones CW, Nair S. Solvothermal deposition and characterization of magnesium hydroxide nanostructures on zeolite crystals. Microporous Mesoporous Mater. 2011;139:120–9.
19. Gong H, Lee SS, Bae T-H. Mixed-matrix membranes containing inorganically surface-modified 5A zeolite for enhanced CO_2/CH_4 separation. Microporous Mesoporous Mater. 2017;237:82–9.
20. Sircar S. Basic research needs for design of adsorptive gas separation processes. Ind Eng Chem Res. 2006;45:5435–48.
21. Chuah CY, Goh K, Bae T-H. Hierarchically structured HKUST-1 nanocrystals for enhanced SF_6 capture and recovery. J Phys Chem C. 2017;121:6748–55.
22. Wee LH, Lohe MR, Janssens N, Kaskel S, Martens JA. Fine tuning of the metal–organic framework $Cu_3(BTC)_2$ crystal size in the 100 nm to 5 micron range. J Mater Chem. 2012;22:13742–6.
23. Rahmani M, Kazemi A, Talebnia F. Matrimid mixed matrix membranes for enhanced CO_2/CH_4 separation. J Polym Eng. 2016;36:499–511.
24. Ewa Ł, Cezary W, Andrzej C, Konrad D, Stanisława S, Anna C, Grażyna C. Preparation of sulfonated polysulfone membrane for enzymes immobilisation. Biocybern Biomed Eng. 2012;32:77–86.
25. Goh P, Ismail A, Sanip S, Ng B, Aziz M. Recent advances of inorganic fillers in mixed matrix membrane for gas separation. Sep Purif Technol. 2011;81:243–64.
26. Zhang Y, Musselman IH, Ferraris JP, Balkus KJ Jr. Gas permeability properties of Matrimid® membranes containing the metal-organic framework cu–BPY–HFS. J Membr Sci. 2008;313:170–81.
27. Adams R, Carson C, Ward J, Tannenbaum R, Koros W. Metal organic framework mixed matrix membranes for gas separations. Microporous Mesoporous Mater. 2010;131:13–20.
28. Car A, Stropnik C, Peinemann K-V. Hybrid membrane materials with different metal–organic frameworks (MOFs) for gas separation. Desalination. 2006;200:424–6.
29. Jeazet HBT, Staudt C, Janiak C. A method for increasing permeability in O_2/N_2 separation with mixed-matrix membranes made of water-stable MIL-101 and polysulfone. Chem Commun. 2012;48:2140–2.
30. Rodrigues MA, de Souza Ribeiro J, de Souza Costa E, de Miranda JL, Ferraz HC. Nanostructured membranes containing UiO-66 (Zr) and MIL-101 (Cr) for O_2/N_2 and CO_2/N_2 separation. Sep Purif Technol. 2018;192:491–500.
31. Perez EV, Balkus KJ Jr, Ferraris JP, Musselman IH. Mixed-matrix membranes containing MOF–5 for gas separations. J Membr Sci. 2009;328:165–73.